Design of Nanostructured Peptoid Assemblies as Synthetic Analogues of Natural Carbonic Anhydrases

Xuansheng Wang

A thesis

submitted in partial fulfillment of the

requirements for the degree of

Master of Science

University of Washington

2025

Committee:

Chun-Long Chen

Robert E. Synovec

Program Authorized to Offer Degree:

Chemistry

University of Washington

Abstract

Design of Nanostructured Peptoid Assemblies as Synthetic Analogues of Natural Carbonic Anhydrases

Xuansheng Wang

Chair of the Supervisory Committee:

Chun-Long Chen

Chemistry

In recent years, the rising carbon dioxide concentration worldwide has become a significant focus of scientific research. Carbon capture represents a feasible solution to the reduction of atmospheric CO_2 and carbonic anhydrase functions as a natural carbon dioxide hydrase to hydrate carbon dioxide efficiently. However, carbonic anhydrase (CA) encounters multiple extraction and preservation difficulties and can easily become inactivated. Thus, development of mimics of carbonic anhydrase has become the focus of substantial research activity. Herein, we developed metal-containing nanosheets as mimics of natural carbonic anhydrase through the incorporation of

metal-ligand active sites into nanostructured peptoid materials. We further assessed their CA mimic performance under different conditions. Our results show that metal-containing peptoid nanosheet materials are effective as CA mimics, which makes them suitable candidates for bioinspired carbon capture.

TABLE OF CONTENTS

Chapter1: INTRODUCTION

1.1 Global warming caused by excessive carbon dioxide emissions and solutions

With the development and progress of society, people's demand for fossil fuels is increasing daily, and carbon dioxide is being excessively emitted. The greenhouse effect caused by excessive carbon dioxide emissions has become a serious problem that people have to face. Excessive emissions of carbon dioxide in the stratosphere will damage the ozone layer. In the past 200 years, the carbon dioxide in the stratosphere has increased by 30% to 31%.[1] According to scientists' speculation, if greenhouse gas emitting countries do not limit the emission of greenhouse gases, the temperature will rise by 4°C by the end of this century.[2] Carbon capture and storage are the best ways to deal with excessive carbon dioxide emissions. There are many ways to achieve carbon capture, as shown in Figure 1.[3] Enzymatic conversion of CO2 into other stable compounds is the most promising technology for environmental protection. In this paper, we will focus on the development of synthetic materials to promote the hydration reaction of carbon dioxide ($CO_2 + H_2O \rightleftharpoons HCO_3^- + H^+$). And the hydration reaction has been widely used for carbon capture and storage.[4] Usually, the hydration reaction of carbon dioxide can be carried out without a catalyst, but this will result in slow hydrate formation.[5] Therefore, a catalyst becomes a necessary choice. Among them, carbonic anhydrase (CA) are valuable zinc-containing metalloenzymes with high catalytic activity and can effectively catalyze the hydrolysis of carbon dioxide.[6]

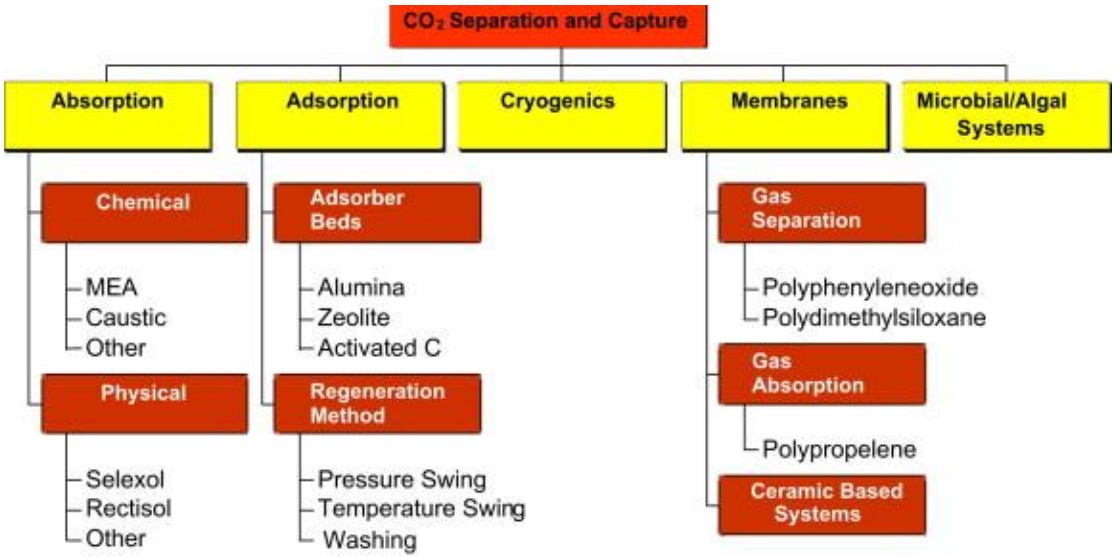

Figure 1 Technical options for CO_2 capture [3]

1.2 Carbonic Anhydrase and Hydration Reactions

Carbonic anhydrase (CA), a very common zinc metalloproteinase, has proven to be a very effective catalyst for CO_2 hydration. In the hydration reaction, CA can well catalyze the conversion between carbon dioxide and water and between bicarbonate and hydrogen ions. There are currently six known CA species from different gene families, which can be classified as α-, β-, γ-, δ-, ζ-, η-, θ CAs.[7] Among them, CA II of the α family has been proven to be a good research object.[8] Figure 2 shows its catalytic principle. [9] In the hydration reaction of carbon dioxide, first, the water

molecule dissociates into protons and hydroxyl ions in a neutral environment, then the carbon dioxide molecule binds to the active site, and then the hydroxyl ion attacks the carbonyl of CO_2 to produce bicarbonate ions (HCO_3^-), and finally the bicarbonate ions (HCO_3^-) are released to regenerate the enzyme (Figure 3).[9]

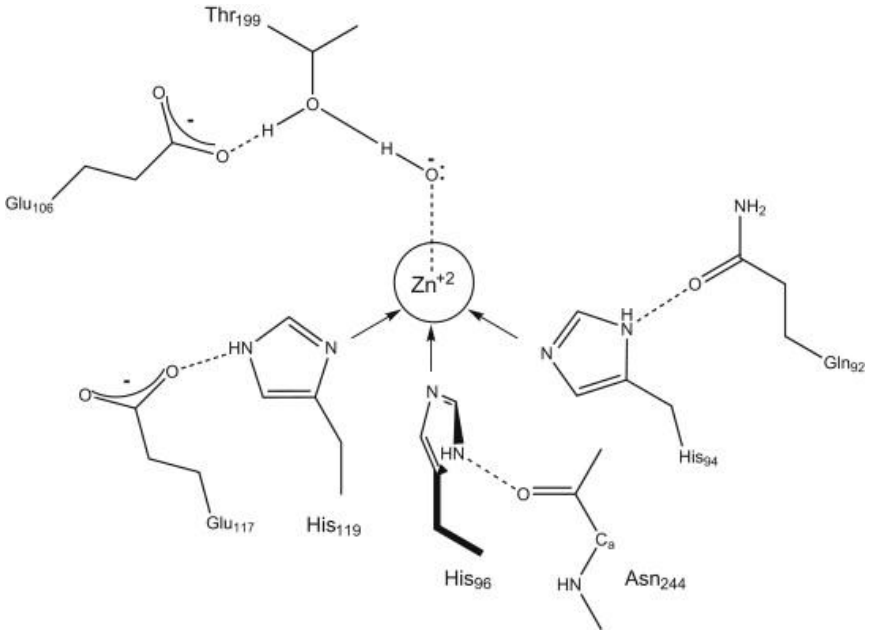

Figure2 Human CA II active site details [10]

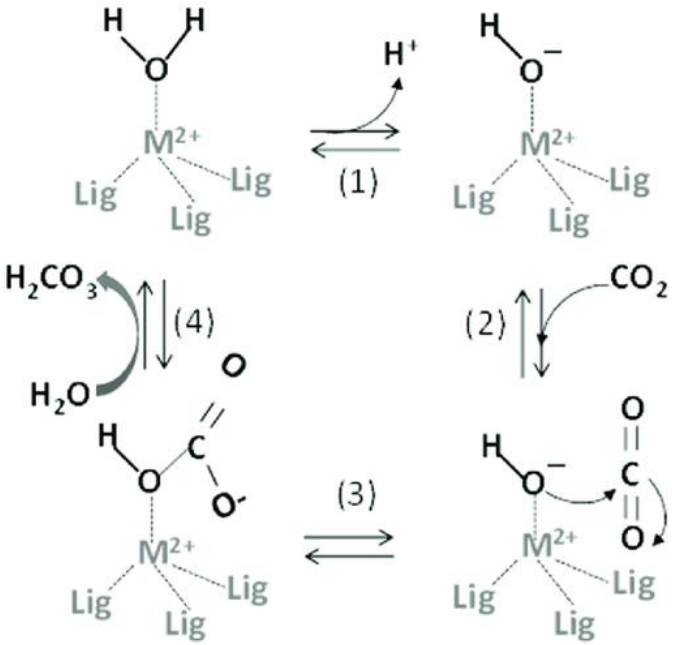

CA class	Lig
α CA	His, His, His
β CA	His, Cys, Cys
γ CA	His, His, His
δ CA	His, His, His
ζ CA	His, Cys, Cys
η CA	His, His, Gly

Figure 3 Carbon dioxide hydration reaction mechanism of Zn-CA II [9]

Although natural CA II has beneficial effects on the hydration reaction of carbon dioxide, it presents significant challenges for industrial carbon capture applications. As a biological enzyme, it takes much effort to extract it from other eukaryotic organisms such as algae, plants, fungi, or some bacteria. Since CA is less stable at high temperatures (such as in flue gas) and alkaline pH conditions, therefore, it is necessary to develop alternative catalysts that can be used to have high catalytic activity and high stability.[11]

1.3 Development of CA mimics

In order to address the intrinsic disadvantages of natural CAs, CA mimic has become a necessary choice. Synthetic CA mimics are often very robust and can be easily synthesized at a low cost. Various CA mimics have demonstrated their advantages in controlling their structures, exhibiting high stability, adjustable catalytic efficiency, and retaining stability after exposure to high temperatures and extreme pH environments.[12] These CA mimics contain metal-ligand complexes that mimic the active site of natural carbonic anhydrases (CAs). The active site of natural CA contains a Zn (II) coordinated with three nitrogen atoms from different histidine and one oxygen atom from a hydroxide ion. Based on this structure, many metal-ligand complexes, such as those listed in Figure 4 [13], have been used as metal-ligand active sites that mimic CA enzymes and used as CA mimetics.

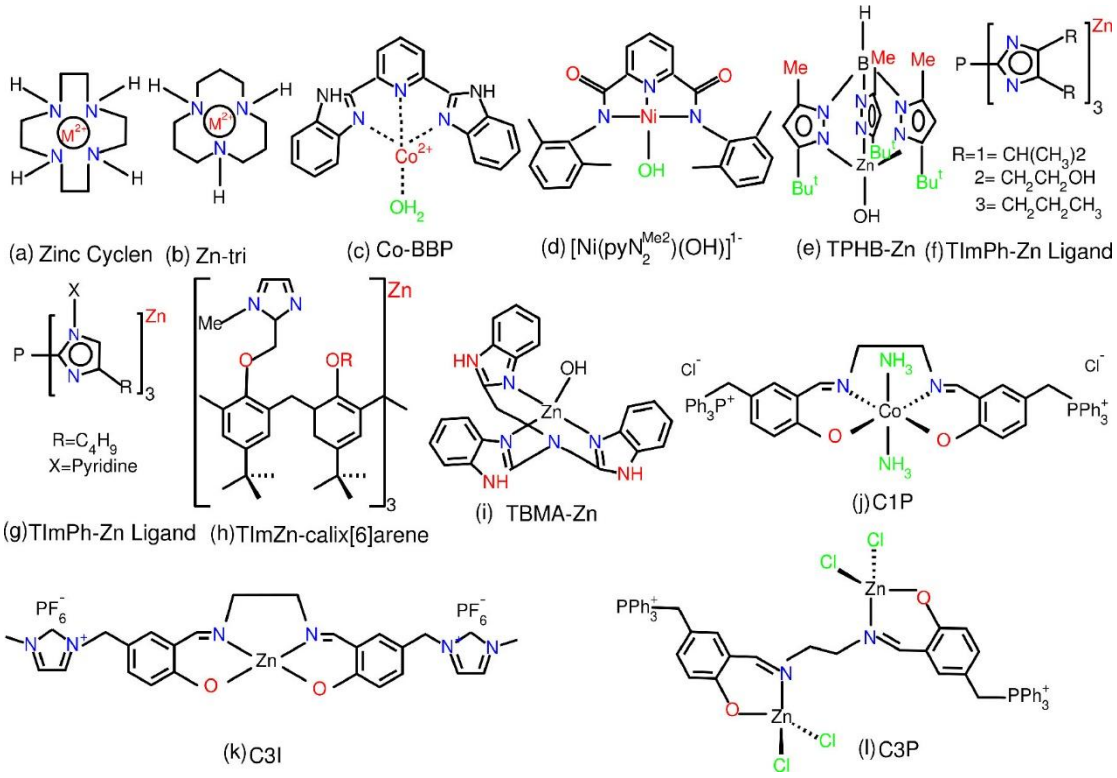

Figure 4 - A list of metal-ligand complexes which have been developed to mimic the active sites of CAs.[13]

Among the above-mentioned CA mimetics, Zn-cyclen is a highly active small molecule CA mimetic. Although the hydration efficiency of Zn-cyclen is relatively slow compared to natural CA, its molecular weight is low, making its activity per unit mass five times lower than that of CA.[14] Through research, Zn-cyclen has also been shown to be effective over a wide pH range and exhibits high thermal stability. Zn-cyclen remain stable at more than 200 degrees.[15] Moreover, the ligand of Zn-cyclen is also mass-produced and commercialized, making it possible to be widely used in industry. Although Zn-cyclen has shown many advantages, it also has some disadvantages. As a soluble enzyme mimic, it is difficult to recycle and reuse. In order to solve these problems, immobilizing CA or CA mimics onto loading support has become a good choice. For example, Zhu et al. fixed CA in alginate polymers by glutaraldehyde cross-

linking, and its activity remained at 56.3% of the original activity. The immobilized CA showed much higher stability than free CA.[16] Figure 5 [17] shows several commonly used immobilization methods: cross-linking, covalent binding, self-assembly, adsorption, co-precipitation, and entrapment. These immobilized CA and CA mimics have improved stability and maintain good catalytic activity under conditions that non-immobilized CAs cannot survive. Furthermore, this enables the easy recycling of these enzymatic materials.[17] Therefore, immobilizing CA mimics is a necessary choice for the widespread application of the carbon dioxide hydration reaction.

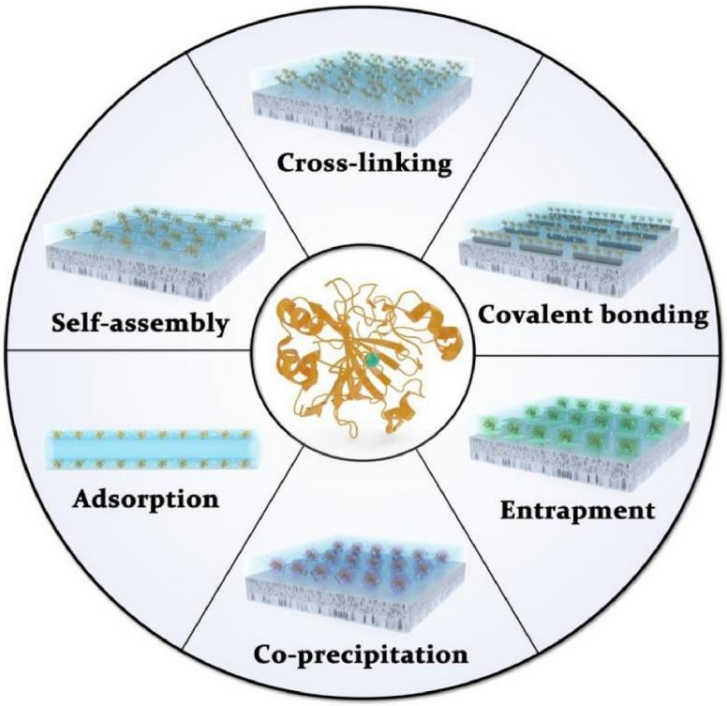

Figure5 Different immobilization approaches for CA based on the membranes. [17]

The self-assembly properties of peptide-based mimetics make them especially interesting because they can create various nanostructures which duplicate the three-dimensional structure of the carbonic anhydrase (CA) active site. [18] The structural complexity and limited stability of peptide-assembled CA mimetics create difficulties

for precise active site microenvironment modulation while maintaining the integrity of self-assembled nanostructures. The existing limitations require researchers to investigate peptidomimetics as a fundamental alternative.

1.4 peptoid.

From the above, we know that peptide-based materials are good candidates for developing CA mimics, but the peptide intra- and inter-molecular interactions are hard to control. Peptoids, that is, poly-N-substituted glycines, are a type of sequence-defined synthetic polymers that have properties bridging natural and non-natural biopolymers. Unlike peptides, peptoids have the side chains connected to the nitrogen atoms of the backbone, instead of the α-carbon (Figure 6).

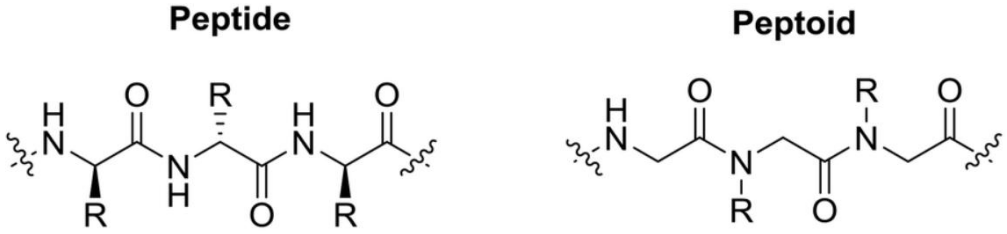

Figure 6 Structures of peptide vs peptoid.

The change in the position of the side chains of peptoids results in the lack of intermolecular hydrogen bonding interactions, which simplifies the control over inter-peptoid interactions, providing unique opportunities for controlled self-assembly.[19] A variety of peptoid sequences have been designed and synthesized for their self-assembly into nanomaterials with various morphologies, [21-27] including nanosheets, and nanotubes (Figure 7) [19,20].

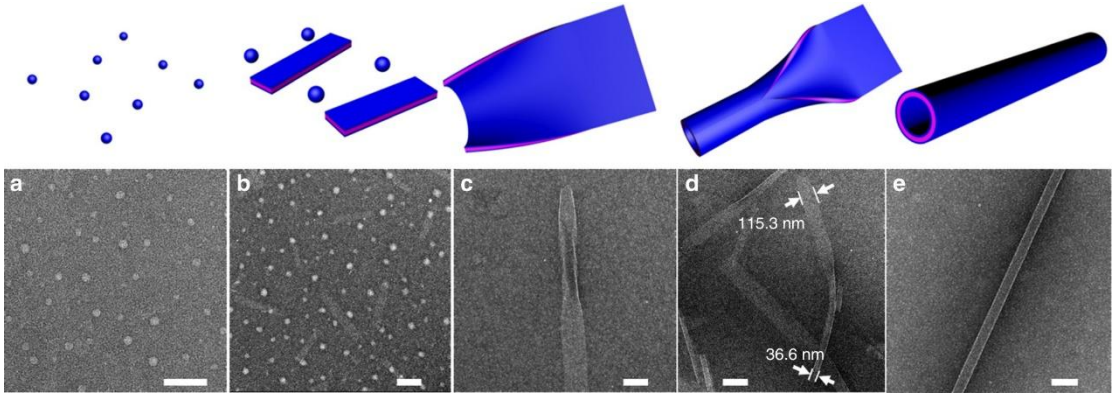

Figure7 Time-dependent TEM images showing the assembly pathway of peptoid nanotubes [20]

The combination of easy synthesis and nanostructure assembly capabilities through controlled processes makes peptoid-based materials highly beneficial. The surface chemical properties of self-assembled nanostructures become precisely controllable through modifications of peptoid sequences. The adjustable nature of peptoids enables them to maintain their structure when exposed to harsh conditions including extreme alkaline pH environments and high temperatures and pure organic solvents. The exceptional peptoid properties include resistance to peptidases/proteases as well as robust chemical and thermal stability.[19] The material properties of peptoid assemlies make them suitable for functional nanomaterials because functional groups can be added to provide specific functionalities.

Thi Kim Hoang Trinh et al. developed self-assembled peptoid nanosheets that mimic natural enzyme active sites to degrade organophosphates. The researchers achieved high catalytic efficiency through metal cation coordination with customized ligands. The researchers optimized the hydrophilic microenvironment surrounding metal-ligand complexes to boost hydrolysis performance.[28] The research demonstrates that peptoid-based assemblies can mimic natural enzyme functions through strategic

modifications of peptoid functional groups. The development of carbonic anhydrase (CA) mimics for CO_2 hydration reactions presents an exciting application based on this concept. A combination of the structural stability of peptoids with the ligand-derived catalytic activity would produce highly efficient synthetic CA-mimic materials. The development of peptoids with accurately arranged side chains to achieve optimal catalytic activity faces significant challenges. This study investigates the use of self-assembled peptoid materials to construct CA mimics for catalytic hydrolysis of p-nitrophenyl acetate (p-NPA).

1.5 CA activity

In my research, the method for evaluating CA activity is colorimetric determination. In this method, we use the hydrolysis p-NPA to evaluate the catalytic activity of CA mimics. The principle is that, in addition to catalyzing the hydration reaction of carbon dioxide, CA can also effectively catalyze the hydration reaction of esters. This study's determination is based on the hydrolysis of 4-Nitrophenyl Acetate to produce 4-Nitrophenol and acetate. 4-Nitrophenol is a color-forming compound that will show yellow in the appropriate solvent, which helps us to use spectrophotometric analysis well. As the reaction proceeds, the absorbance at a wavelength of about 400nm will increase, thereby providing the data required to evaluate CA-like activity.

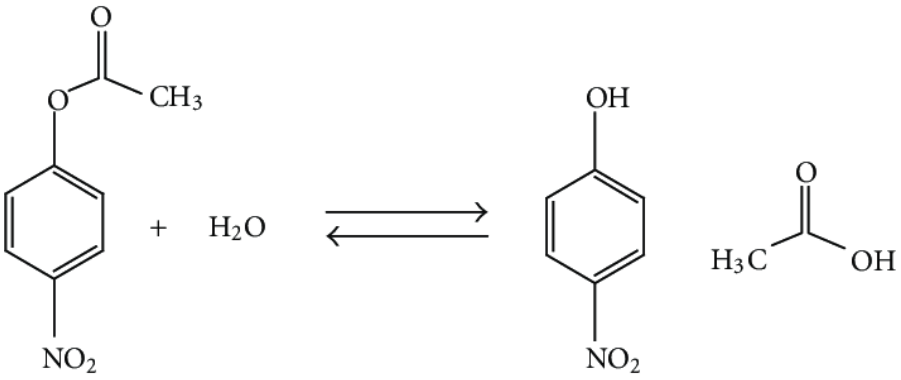

Figure 8: Hydrolysis reaction of para-nitrophenyl acetate (p-NPA) to para-nitrophenol (p-NP) [29]

Chapter 2: Material and method

2.1 Material

All solvents were brought from Fisher or VWR and used without further purification. Bromoacetic acid and Rink Amide resin (0.7-1.0 meq/g) were purchased from Chem-Impex International, Inc. β-alanine tert-butyl ester hydrochloride was purchased from Oakwood Chemical. N, N'-diisopropylcarbodiimide, 4-methylpiperidine, potassium carbonate (K_2CO_3), 4-bromophenyl ethylamine, tert-butyl-N-(2-aminoethyl) carbamate, 2-methoxyethyl amine and trifluoroactic acid (TFA) were purchased from Oakwood Chemical. 8-hydroxyquinoline (Nqn), cobalt (II) tetrafluoroborate hexahydrate ($Co(BF_4)_2$) was purchased from Sigma-Aldrich. All amine submonomers were used as received. 4-nitrophenol (p-NP), 4-nitrophenyl acetate (p-NPA), dichloromethane (DCM), dimethylformamide (DMF), 4-(2-hydroxyethyl)-1-piperazineethanesulfonic acid (HEPES), and LC/MS graded acetonitrile (ACN) were brought from Thermo Scientific. HPLC-grade water was purchased from Sigma-Aldrich. MilliQ water at 18

MΩ cm was used for all experiments.

2.2 peptoid synthesis

All peptoid sequences were synthesized on Rink amide resins using solid-phase synthesis. The 100mg Rink amide resins (0.09 mmol) were first swollen in N, N-dimethylformamide (DMF) for 10 minutes. After that, the resins were filtered, and then 2 mL of 20% (v/v) 4-methylpiperidine/DMF solution was added to remove Fmoc groups. The mixture was then shaken at room temperature by 40 minutes. Then, the resins were drained and washed with DMF using five washes of 1 mL each.

Then, using 1.5 mL of 0.6 M bromoacetic acid and 0.3 mL of a 50/50 (v/v) N, N-diisopropylcarbodiimide (DIC)/DMF mixture to subject the deprotected resin to acylation. The reaction mixture was shaken for 10 minutes at room temperature, followed by washing with DMF (5 × 1 mL). After that, 1.5 mL of a 0.6 M primary amine solution in N-methyl-2-pyrrolidone (NMP) was used to achieve nucleophilic displacement of bromide with the submonomers, and the mixture was agitated for 10 minutes at room temperature. The solution was filtered, and the resins were washed with DMF (5 × 1 mL). The reactions were repeated by using acylation and displacement reactions with primary amines [such as 4-bromophenethylamine (Nbrpe) or tert-butyl (2-aminoethyl)carbamate (Nae)] to obtain the desired target peptoid sequence.

To add 8-hydroxyquinoline (Hqn) to the peptoid, the peptoid was mixed with 1.5 mL of 0.6 M bromoacetic acid and 0.3 mL of 50/50 (v/v) DIC/DMF for 10 minutes, after which the supernatant was removed and washed with DMF (5 × 1 mL). Then, 1.5 mL

of 0.6 M tris(2-aminoethyl)amine in NMP was added to the above-mentioned resin, and the mixture was stirred overnight at room temperature, filtered, and washed with DMF (5 × 1 mL). Furthermore, 1.5 mL of 0.6 M bromoacetic acid and 0.6 mL of 50/50 (v/v) DIC/DMF were used for the acylation cycle. Then 1.5 mL of 0.6 M benzylamine solution in NMP, or 1.5 mL of 0.6 M isopropyl amine solution in NMP, was added, and stirred at room temperature for 10 minutes to allow the bromide to undergo a nucleophilic displacement reaction with the submonomer. The solution was filtered, and the resin was washed with DMF (5 × 1 mL). Then use 3 mL of 0.6 M (bromoacetic acid/bromoacetic -S5 acid) and 0.6 mL of 50/50 (v/v) DIC/ DMF. Finally, 3 mL of 0.6 M NQN in NMP and 200 mg of K_2CO_3 were added to the above resin, and the mixture was stirred at room temperature overnight, filtered, and washed with DMF (5×1 mL).

2.3 peptoid self-assemble

During the self-assembly process, 100 μL acetonitrile was added into the 1.0μmol peptoid sample, which was then heated to 55 ℃ for 24h. Then,100ul DI water was added to it. The pH was adjusted to 7-8. Finally, the mixture was left to evaporate at 4℃.

For the formation of metal-containing peptoid assemblies, I added acetonitrile to the sample for coordination reaction and then mixed the peptoid and metal in acetonitrile in a ratio of 1:1 eq, which resulted in a final volume of 100 μL.[28] Then, I heated the mixture to 55℃ for 24h. Then, 100 μL DI water was added to it. Then, the pH was adjusted to pH 7-8. Finally, the mixture was left to evaporate at 4℃.

2.4 Characterization

Atomic force microscopy (AFM)

Atomic force microscopy (AFM) experiments were performed at room temperature using the Scansys mode of a Bruker Icon. To prepare the AFM sample, 1.0 μL of the peptide self-assembly solution was diluted with 49 μL of deionized water and then dropped onto a freshly exfoliated mica surface and allowed to stand for 10 minutes. The solution on the mica surface was blotted with filter paper and then dry with nitrogen.

2.5 Catalytic activity of peptoid-based CA mimetics

UV-vis measurements

As mentioned before, we can use p-nitrophenol acetate (p-NPA) to evaluate the catalytic activity of peptoid-based CA mimics. For UV-vis testing, we use the Biotek Synergy Lx Multi-mode Reader to perform the test. Specifically, we will first add 255μL of 100mM HEPES buffer (pH=7.4) to the 96-well plate, and then we will add 37.5μl of 1mM self-assembled peptoid solution. The control group is replaced with 37.5 μL of DI water or the same volume of metal solution. Finally, add 7.5 μL of 10 mM PNPA solution before using the instrument.

Standard curve

In order to calculate the conversion rate of p-NPA to p-NP, it is necessary to obtain data for plotting the UV-vis absorbance of a series of p-NP concentrations from 0 to 250μM at 400nM. First, add 255 μL of HEPES buffer to a 96-well plate, and then add different ratios of water and p-NP solution dissolved in acetonitrile. The ratios are shown in Table 1. Then, Biotek Synergy Lx Multi-mode Reader will be used to perform UV-vis measurements in the range of 300-700 to obtain the required data.

Table1 Used to measure the ratio of hydrated p-NP required for different concentrations prepared by standard curve

	100mM HEPES buffer	DI water	10mMp-NP solution
0μM	255μL	37.5μL	7.5μL
50μM	255μL	39μL	6μL
100μM	255μL	40.5μL	4.5μL
150μM	255μL	42μL	3μL
200μM	255μL	43.5μL	1.5μL
250μM	255μL	45μL	0μL

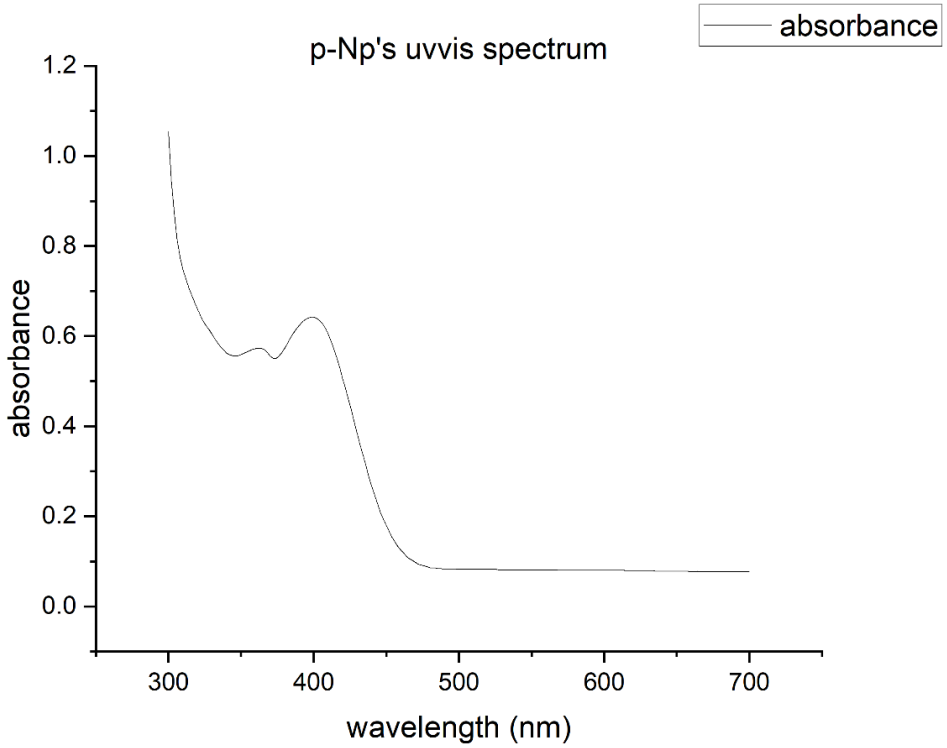

Figure9 The standard curve of 250μM p-NP's solution at pH 7.35

(a)

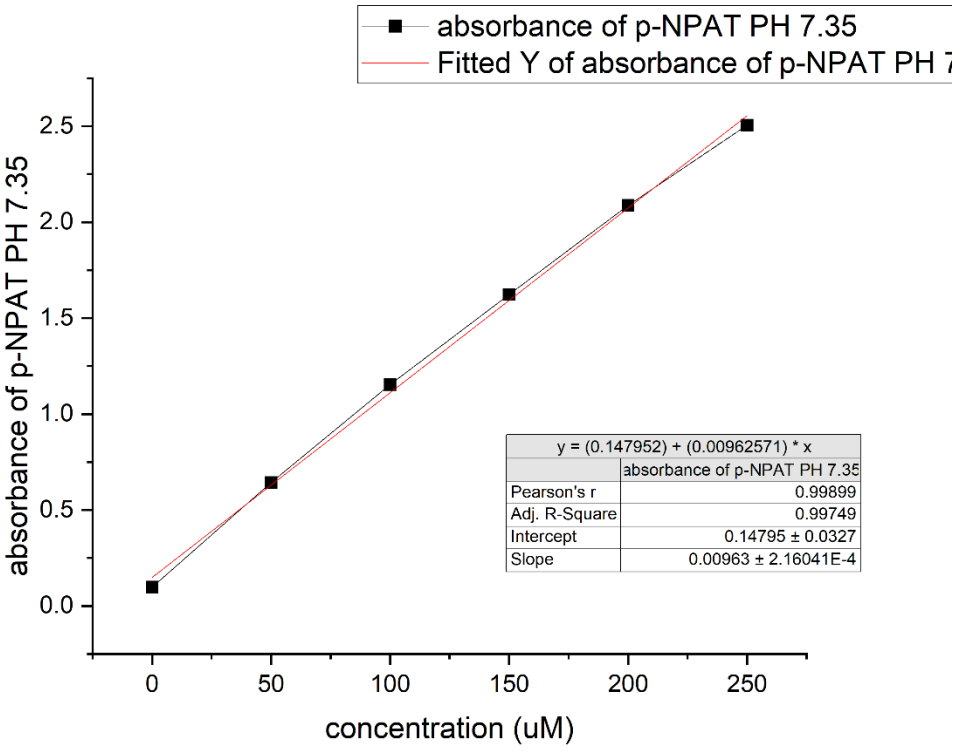

(b)

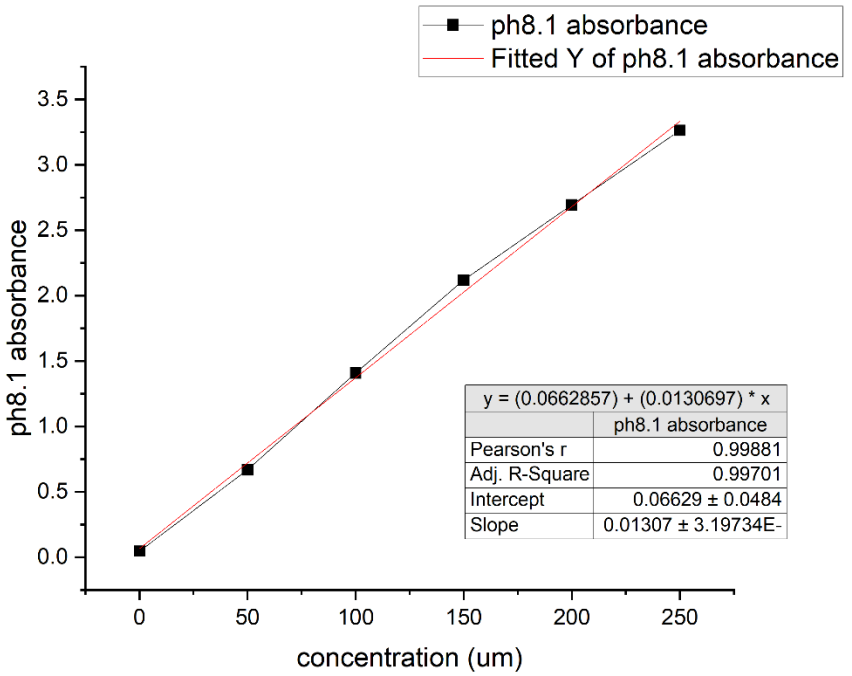

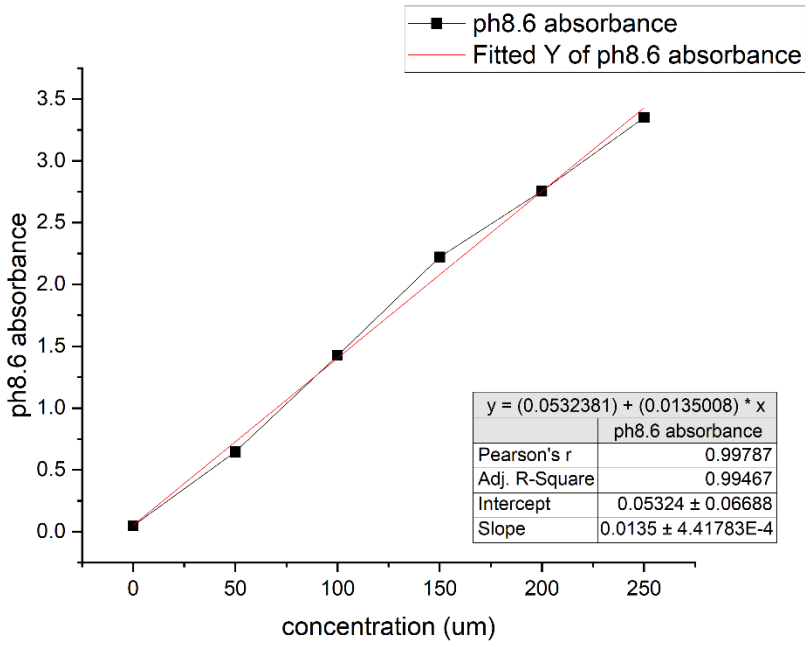

(c)

Figure10 (a)The standard curve of p-NP's solution at PH 7.35 (b) The standard curve of p-NP's solution at pH 8.1 (c) The standard curve of p-NP's solution at pH 8.65

Chapter3: RESULTS AND DISCUSSION

3.1 Peptoid self-assembly and characterization

As mentioned in the introduction, we are developing a CA-mimic catalyst using self-assembled peptoid materials. To this end, we designed and synthesized a peptoid with three regions: the hydrophobic region, the hydrophilic region, and a terminal coordination site. First, the hydrophobic region contains six N-([2-(4-bromophenyl) ethyl] glycine) groups (Nbrpe). The π-π interactions between the aromatic groups allow the peptoid to freely self-assemble into nanotubes or nanosheets [30]. The hydrophilic region contains six N-(2-aminoethyl)glycine (Nae) units. The ligand domain is the most important. We tested it with two different groups. The first peptoid's ligand is an 8-hydroxyquinoline (Nqn) group adjacent to Npm [Npm = N-(1-phenylmethyl) glycine], and the other is a peptoid with a Nip [Nip = N-(isopropyl)glycine] group instead of NPM. It can partially coordinate the transition metal and the nitrogen and oxygen atoms in the ligand to obtain a structure similar to the CA active site. Adding ligands to the peptoid can obtain sufficient stability after the peptoid self-assembly. Moreover, try to study the difference in catalytic activity caused by the difference in ligand parts.

The reason why I chose these two peptoids is that they both have the same hydrophobic domain, hydrophilic domain, and ligand domain. This can effectively control the differences between the peptoids. The difference between Pep-1 and Pep-2 is that Pep-1 has two Npm groups near the Nqn group. At the same time, Pep-1 replaces the Npm group with two Nipa groups. Moreover, the reason why I tried to do those two groups is that those two parts could influence the catalysis.[28] I know that the local

hydrophobic environment can control substrate binding, and it will contribute significantly to the catalytic efficiency.[31]

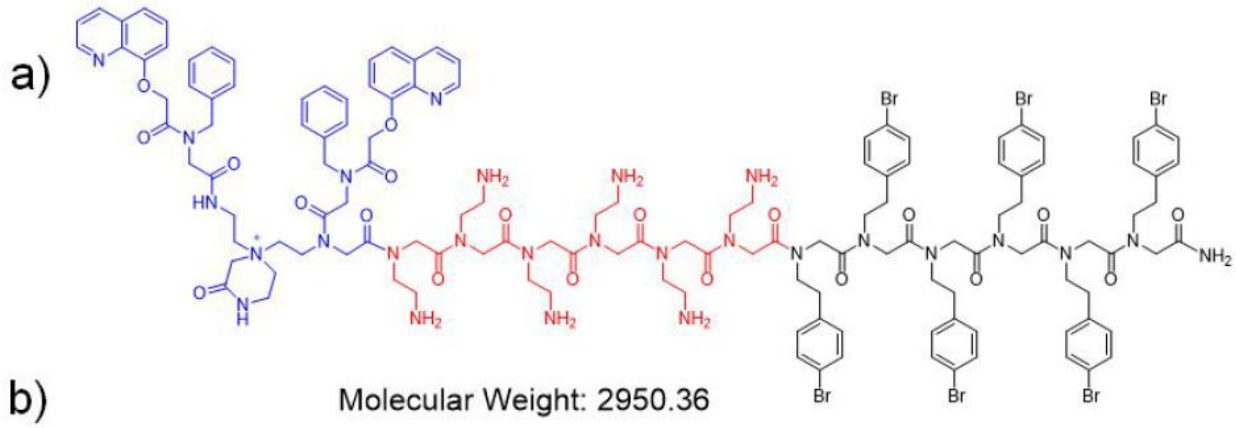

Figure 11: Chemistry structure for peptoid-1 $(Nbrpe)_6(Nae)_6Npm_2Nqn_2$

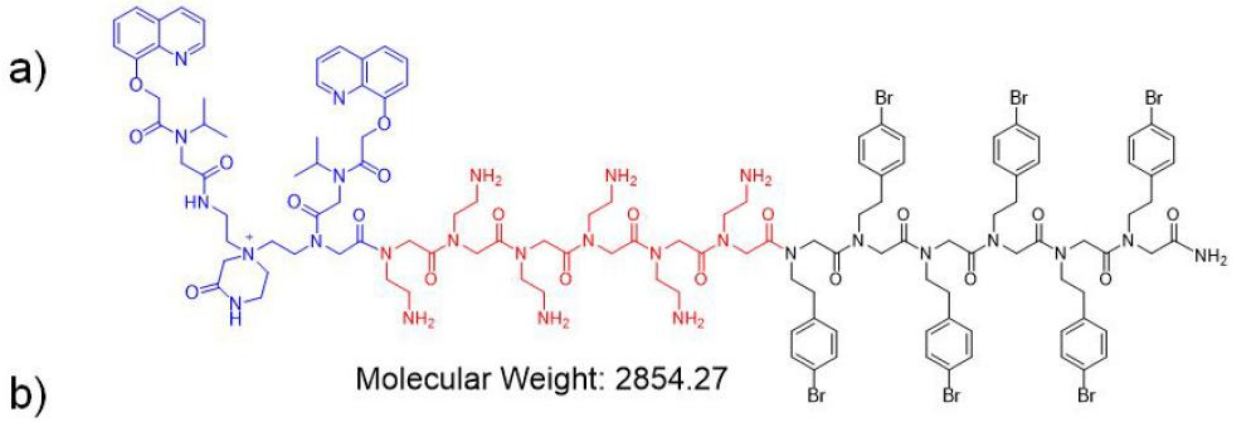

Figure 12: Chemistry structure for peptoid-2 $(Nbrpe)_6(Nae)_6Nip_2Nqn_2$

To prepare the peptoid I needed, we added acetonitrile to the sample for the coordination reaction and then mixed the peptoid and metal in acetonitrile in a ratio of 1:1 eq. Then, we heated the mixture to 55°C for 24 hours. Then, water was added to it. The pH was adjusted to 7-8. Finally, the mixture was left to evaporate at 4°C.

After this, we need to use AFM to characterize the sample. We first take one μL of peptide self-assembly solution from the sample, dilute it with 49 μL of deionized water, then drop it on the newly peeled mica surface and let it stand for 10 minutes. Use filter

paper to absorb the solution on the mica surface, then dry it with nitrogen. As we can see in Figure 13, all the samples formed nanosheets.

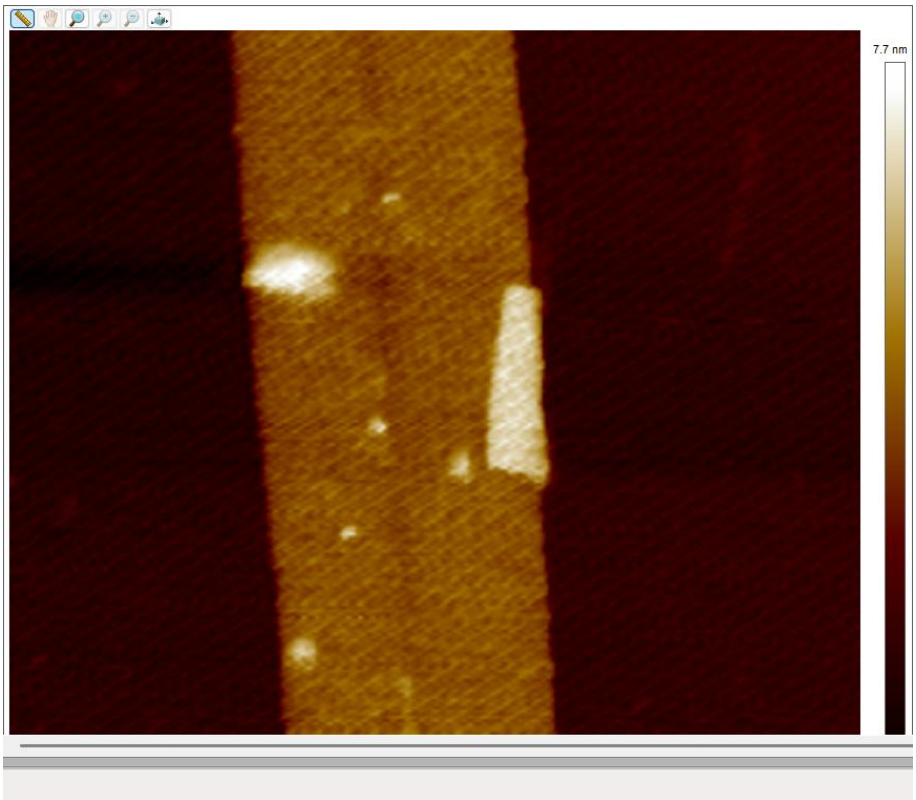

Figure 13: AFM images of Pep-1 and Pep-2 nanosheets.

3.2 Catalytic activity of peptoid assemblies of Pep-1 And Pep-2

In order to evaluate the catalytic effect of CA mimics composed of Pep-1 or Pep-2, we used the hydrolysis of p-NPA. In the hydrolysis test, after p-NPA is added to the peptoid solution containing 100 mM HEPES buffer, the solution will become longer with the increase of time, and the color will gradually turn yellow, and the yellow color indicates that p-NPA has been effectively degraded in the peptoid-based CA mimics. Therefore, measuring the UV-visible absorbance of the solution at 400nm every 15 minutes can provide us with the absorbance of p-NP at each time, and according to the standard curve of p-NP measured previously, the conversion rate of Pep-1 and Pep-2 can be

obtained.

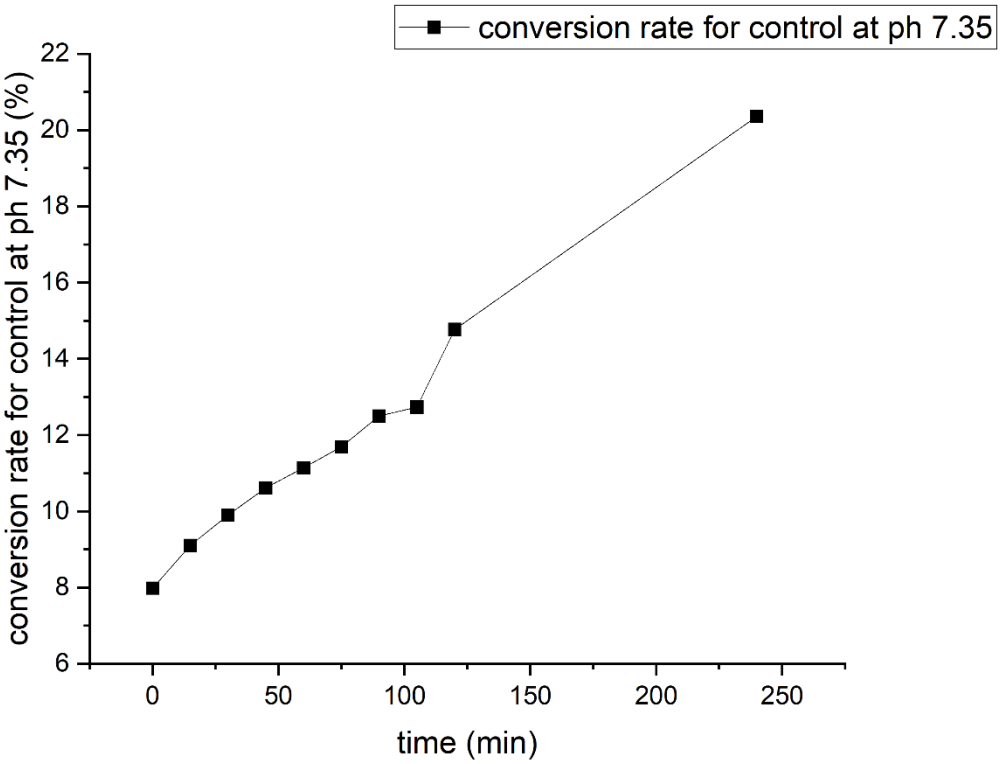

Figure 15: control's conversion rate at ph 7.35

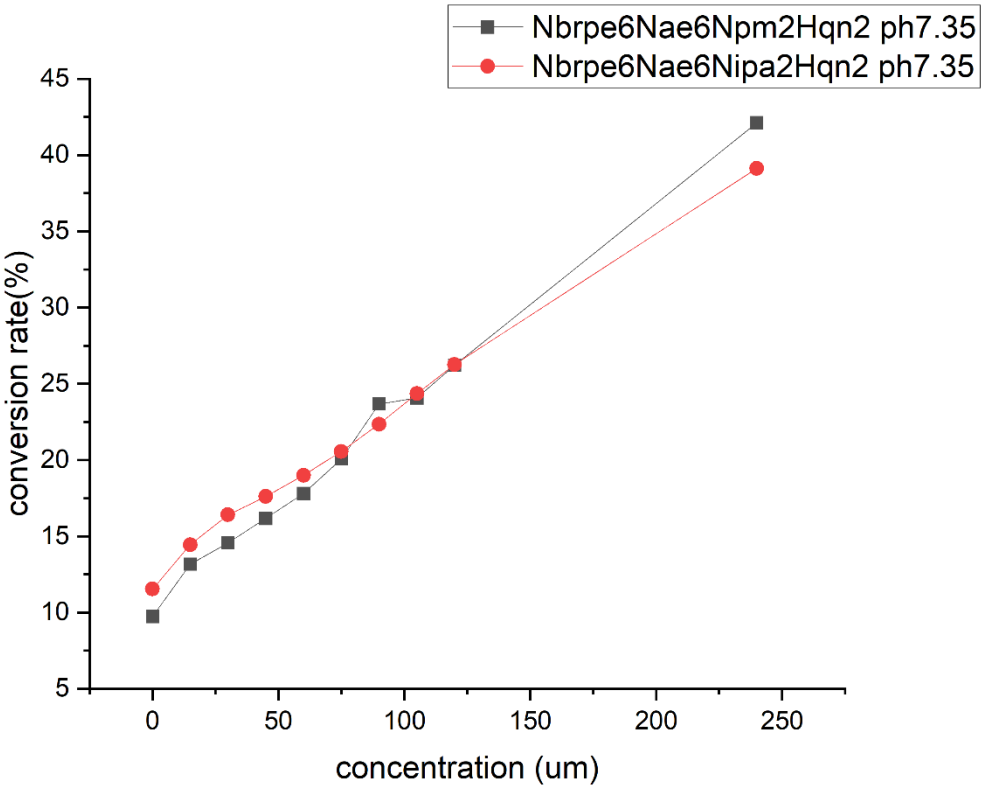

Figure 16: Pep-1 and Pep-2's conversion rate at PH 7.35

As shown in the figure above, Pep-1 and Pep-2 showed a specific catalytic effect at pH 7.35, but compared with the control in Figure 15, the catalytic effect was still not apparent. After 4 hours of catalytic reaction, the conversion rate of Pep-1 was 42%, while the conversion rate of Pep-2 was 39%. In the control, no peptoid was added, and DI water was used instead of peptoid; there was still a 20% catalytic effect. Compared with the control, Pep-1 and Pep-2 did not show the excellent catalytic performance of other products under the same pH environment.

As mentioned above, Pep-1 and Pep-2 do not have a good catalytic effect at a pH of 7.35. Therefore, it is necessary to test the catalytic effect of Pep-1 and Pep-2 at a pH greater than 8. This is because Nucleophilic Hydroxide (OH^-) concentration will

increase significantly as the pH value increases. As a nucleophilic reagent, OH^- will attack the substrate, so a higher concentration of OH^-, i.e., a high pH environment, will accelerate hydrolysis and improve catalytic efficiency.[32]

Therefore, in order to test the catalytic activity of Pep-1 and Pep-2 under different pH environments, we need to prepare buffers with different pH values for hydrolysis tests. In this part, we add 255 μL of HEPES buffer diluted from 1M to 100 mM and adjusted to pH 8.1 and 8.6 in a 96-well plate, then add 37.5 μL of peptoid solution and 7.5 μL of p-NPA solution before the test. Then put it into the plate reader to read the data within 4 hours and obtain the required data based on the absorbance at 400nm.

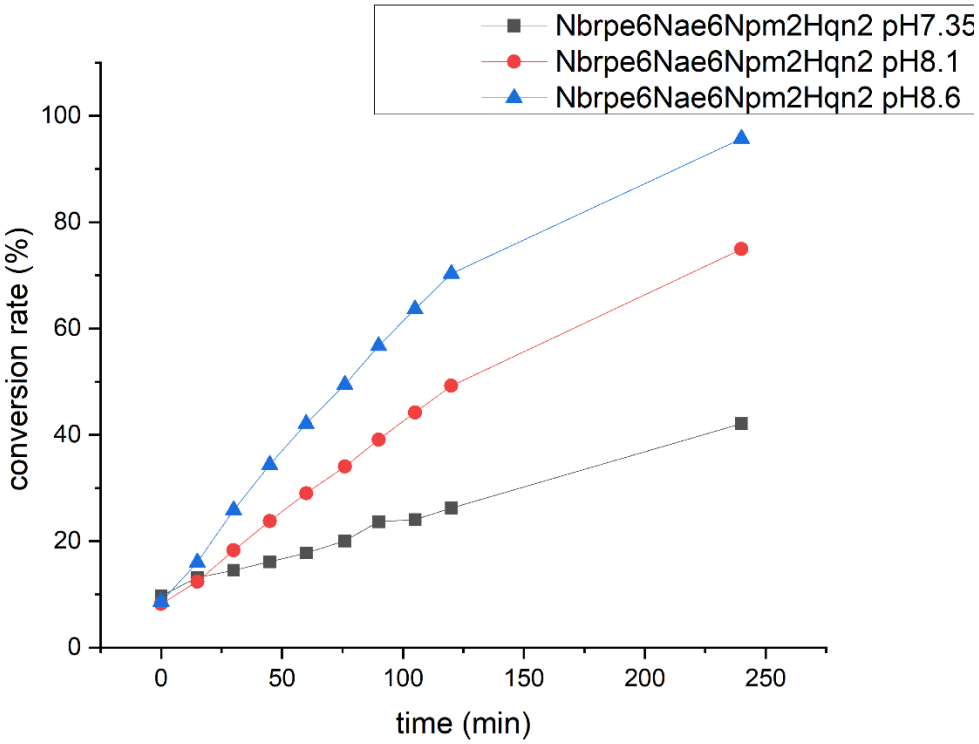

Figure 17: the conversion rate for Pep-1 at different pH,

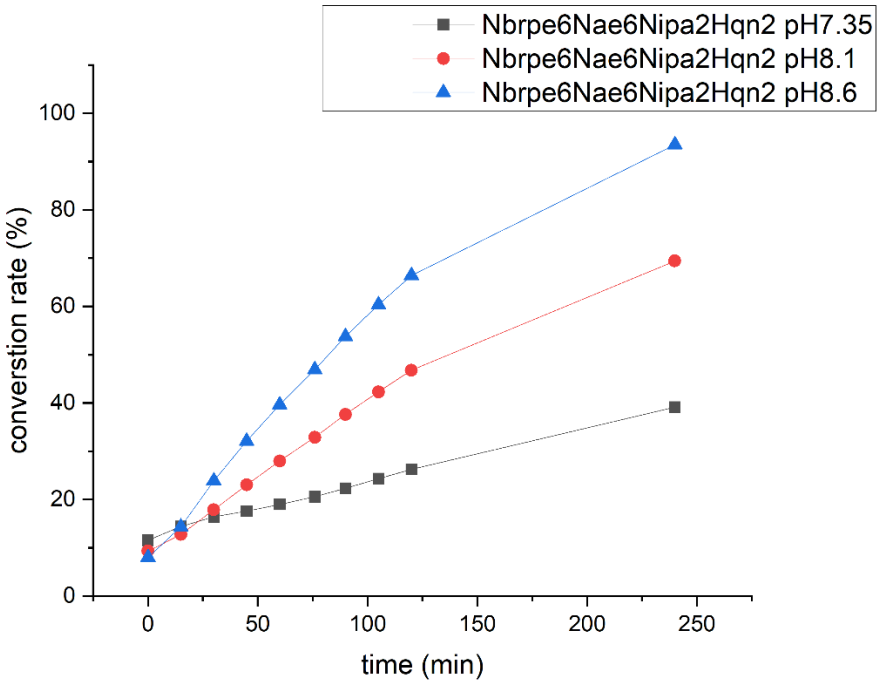

Figure 18: conversion rate for Pep-2 at different pH

As shown in Figures 17 and 18, the pH environment has a certain effect on the hydrolysis activity of the peptoid CA mimetic on p-NPA, and its catalytic effect increases with the increase of the pH environment, indicating that the pH environment plays an important role in the hydrolysis of p-NPA.

3.3 Effects of metal binding of Pep-1 and Pep-2 on hydrolysis

As mentioned above, CA mimics have different mimic structures such as Zn-cyclen, Zn-tri, and there are also mimics composed of other metals such as 2,6-bis(2-benzimidazolyl) pyridine cobalt complex, (Co-BBP). Therefore, I also tried to combine Pep-1 and Pep-2 with Co^{2+} to test their effect on hydrolysis.

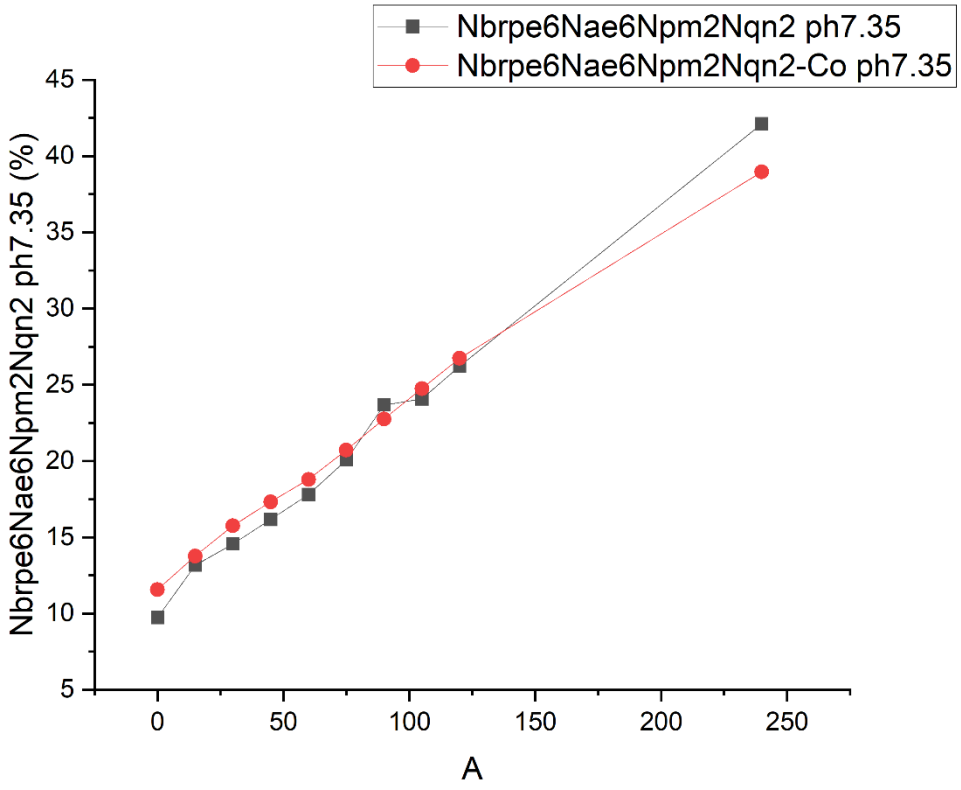

Figure 19: Pep-1 and Pep-1-Co's conversion rate at pH 7.35'

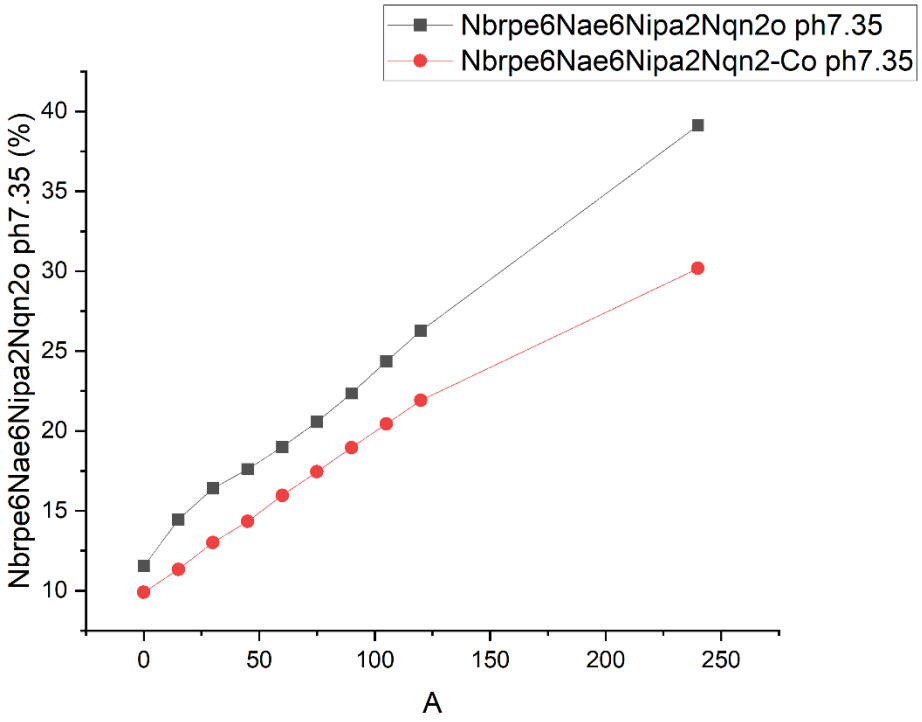

Figure 20: Pep-1 and Pep-1-Co's conversion rate at pH 7.35

The figure shows that at pH 7.35, Pep-1 (metal-free) and Pep-1-Co (metal-bound) showed equivalent catalytic performance within the first two hours of the experiment. The catalytic efficiency of Pep-1 (metal-free) reached 42.12% after four hours, but Pep-1-Co failed to show the same degree of improvement. Under the same experimental conditions, the conversion efficiency of Pep-2 reached 39.12% when using the metal-free form, but only 30.18% when using the metal-bound variant (Pep-2-Co). The two peptoid variants (Pep-1 and Pep-2) have the same hydrophilic domain, hydrophobic domain, and ligand domain, so the experimental results only depend on the presence or absence of metal coordination.

Therefore, we assume that the enhanced catalytic efficiency of non-metallic peptoids (Pep-1 and Pep-2) comes from the structural flexibility of their ligand domains because they are not restricted by metal coordination. In the absence of metal binding, the ligand domain maintains a flexible structure, allowing it to adapt to substrate binding through subtle structural rearrangements. In metal-binding peptoid nanomaterials (Pep-1-Co and Pep-2-Co), coordination with metal ions may limit conformational adjustments, thereby hindering substrate binding.

3.4 Effect of ultrasonic treatment on the catalytic effect of Pep-1 and Pep-2 assemblies

Through the above experimental tests, we know that the catalytic effect of Pep-1 and Pep-2 peptoid assemblies will be affected by pH concentration and whether they are bound to metals. In order to explore other conditions that affect the catalytic effect of

Pep-1 and Pep-2, we tried to use ultrasonic treatment of solutions containing Pep-1 and Pep-2 assemblies to test their effect on the catalytic effect. Because sonication is a process that uses high-frequency sound waves (ultrasound) to agitate particles and disrupt cells, tissues, or q ,[33,34] we expect that ultrasonic treatment should be able to cut these self-assembled Pep-1 and Pep-2 Nanosheets into smaller fragments, thereby increasing the surface area. We speculate that the increase in surface area may make the interaction between the mimic and the substrate stronger, resulting in more frequent collisions, which in turn increases the final reaction rate. Therefore, before conducting a conventional hydrolysis test, we will take out the required volume from the 1mM solution and put it into a centrifuge tube, put it into an ultrasonic instrument to perform ultrasonic treatment on Pep-1 and Pep-2 nanosheets for 1 hour and 4 hours, and then put it into a plate reader for a 2-hour UV-vis test.

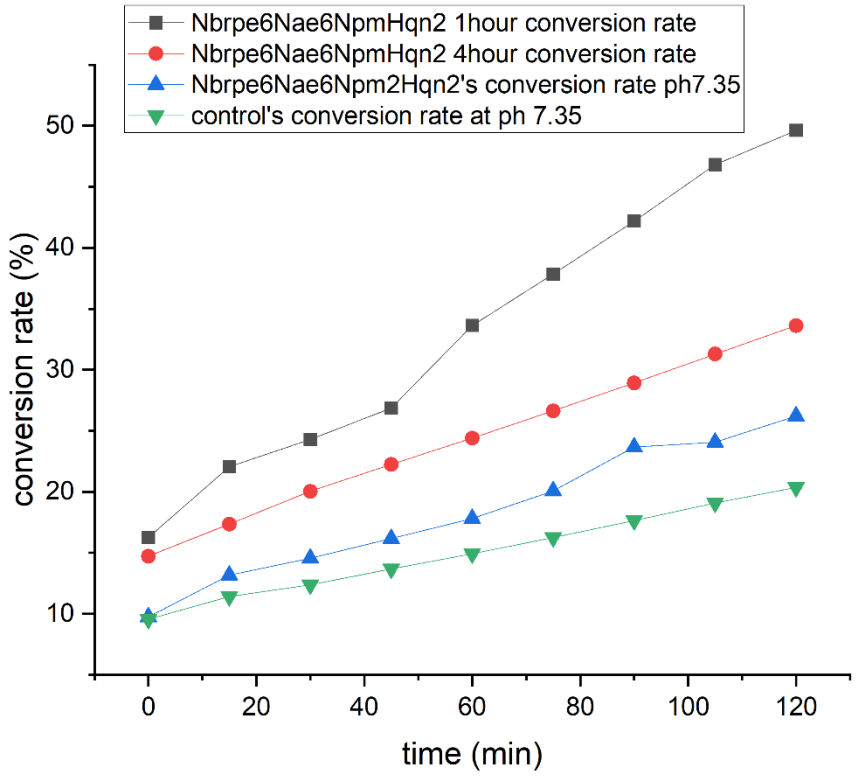

Figure 21: Conversion rate using sonication-cutting Pep-1 nanosheets

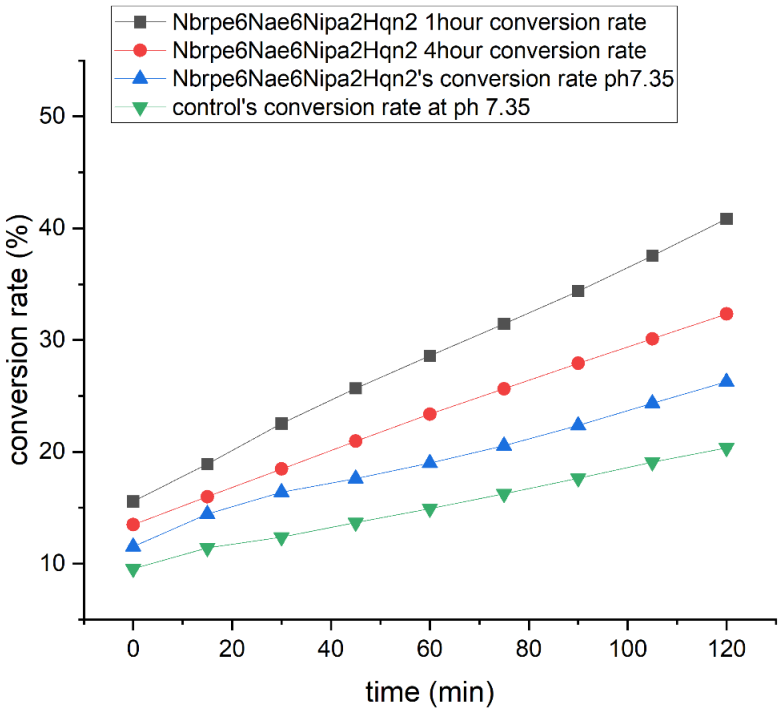

Figure 22: Conversion rate using sonication-cutting Pep-2 nanosheets

As can be seen from the data shown in Figures 22 and 23, ultrasonic treatment significantly improved the catalytic performance of Pep-1 and Pep-2 nanosheets. Using deionized water (DI) as a control and compared with untreated peptoid solutions, the hydrolysis results showed that the catalytic activity was significantly improved after one hour of ultrasonic treatment. Specifically, under these conditions, the catalytic efficiency of Pep-1 increased to 49.6%, while the catalytic efficiency of Pep-2 reached 40.8%. However, extending the ultrasonic treatment time to four hours produced the opposite result: the catalytic effect of both peptoids decreased, and the catalytic efficiency of Pep-1 and Pep-2 increased by only 33.63% and 32.3%, respectively.

These findings suggest that while ultrasonic treatment can initially enhance catalytic activity, prolonged exposure to ultrasound may reduce its catalytic effect. AFM results of these peptoid nanosheets after sonication for 1hour and 4 hour suggest that, ultrasonic treatment breaks the Pep-1 and Pep-2 nanosheets into smaller particles, thereby increasing their surface area and promoting the interaction of the mimic with the substrate in the first hour. This is consistent with our hypothesis that a larger surface area promotes more frequent collisions between the enzyme-mimetic peptoid and the substrate, thereby accelerating the reaction rate. However, after four hours of sonication, the nanosheets may be excessively fragmented, which may reduce their structural integrity or stability, ultimately weakening their catalytic ability.

Chapter4: Conclusion

In this study, we designed and synthesized peptoid-based nanomaterials as CA mimics from the self-assembly of two different peptoids, which contain three parts: a

hydrophobic domain, a hydrophilic domain, and a ligand domain that can bind to Co^{2+} ions. We investigate the influence of peptoid nanomaterial morphology on the catalytic hydrolysis reaction. According to the results, we can conclude that the Npm group may interact with p-NPA through π–π interactions, which increases its hydrolysis effect and makes it have a better catalytic effect than $Nipa_2$ group. Increasing the pH concentration of the peptoid solution and ultrasonic treatment are also good ways to improve the catalytic effect. We verified that the nanomaterials assembled from these two peptoids have good catalytic effects on the hydration reaction of carbon dioxide. Because peptoids are highly stable and peptoid-based nanomaterials are highly programmable, we believe that peptoid-based CA mimetics offer great potential in CO_2 hydration, thereby facilitating the capture and storage of CO_2.

Chapter5. Acknowledgement

This work was supported by the US Department of Energy (DOE), Office of Science, Office of Basic Energy Sciences (BES) under an award FWP 80124 at Pacific Northwest National Laboratory (PNNL).

Part of AFM experiments were conducted at the Molecular Analysis Facility, a National Nanotechnology Coordinated Infrastructure (NNCI) site at the University of Washington, which is supported in part by funds from the National Science Foundation (awards NNCI-2025489, NNCI-1542101).

I am also very grateful to Professor Chen for his guidance and help throughout my

graduate project. I am also very grateful to Thi kim Hoang Trinh for his guidance on the peptide sample and Progyateg Chakma for his guidance on the hydrolysis test. And I also grateful for ling Dai, Renyu Zheng, and Yifeng Cai’s help

Bibliography

(1)Kabir, M.; Habiba, U. E.; Khan, W.; Shah, A.; Rahim, S.; Farooqi, Z.-U.-R.; Muhammad Zafar Iqbal; Shafiq, M. Climate Change due to Increasing Concentration of Carbon Dioxide and Its Impacts on Environment in 21st Century; a Mini Review. *Journal of King Saud University - Science* **2023**, *35* (5), 102693–102693. https://doi.org/10.1016/j.jksus.2023.102693.

(2)Nataly Echevarria Huaman, R.; Xiu Jun, T. Energy Related CO2 Emissions and the Progress on CCS Projects: A Review. *Renewable and Sustainable Energy Reviews* **2014**, *31*, 368–385. https://doi.org/10.1016/j.rser.2013.12.002.

(3)Rubin, E. S.; Mantripragada, H.; Marks, A.; Versteeg, P.; Kitchin, J. The Outlook for Improved Carbon Capture Technology. *Progress in Energy and Combustion Science* **2012**, *38* (5), 630–671. https://doi.org/10.1016/j.pecs.2012.03.003.

(4)Hu, Q.; Xiao, X. Formation Methods and Applications of Carbon Dioxide Hydrate: An Overview. *Carbon Capture Science & Technology* **2023**, *7*, 100113. https://doi.org/10.1016/j.ccst.2023.100113.

(5)Azam, M. Z.; Xin, F. Speedy Hydration of Carbon Dioxide Hydration in an Immediate Coolant of Ice Granules. *ACS Omega* **2021**, *6* (2), 1083–

1092. https://doi.org/10.1021/acsomega.0c03327.

(6)Ren, S.; Jiang, S.; Yan, X.; Chen, R.; Cui, H. Challenges and Opportunities: Porous Supports in Carbonic Anhydrase Immobilization. *Journal of CO2 Utilization* **2020**, *42*, 101305. https://doi.org/10.1016/j.jcou.2020.101305.

(7)Kumar, S.; Rulhania, S.; Jaswal, S.; Monga, V. Recent Advances in the Medicinal Chemistry of Carbonic Anhydrase Inhibitors. *European Journal of Medicinal Chemistry* **2020**, *209*, 112923. https://doi.org/10.1016/j.ejmech.2020.112923.

(8)Kim, J. K.; Lee, C.; Lim, S. W.; Adhikari, A.; Andring, J. T.; McKenna, R.; Ghim, C.-M.; Kim, C. U. Elucidating the Role of Metal Ions in Carbonic Anhydrase Catalysis. *Nature Communications* **2020**, *11* (1), 4557. https://doi.org/10.1038/s41467-020-18425-5.

(9)Lionetto, M.; Caricato, R.; Giordano, M.; Schettino, T. The Complex Relationship between Metals and Carbonic Anhydrase: New Insights and Perspectives. *International Journal of Molecular Sciences* **2016**, *17* (1), 127. https://doi.org/10.3390/ijms17010127.

(10)Crichton, R. R. Zinc – Lewis Acid and Gene Regulator. *Biological Inorganic Chemistry* **2012**, 229–246. https://doi.org/10.1016/b978-0-444-53782-9.00012-7.

(11)Talekar, S.; Jo, B. H.; Dordick, J. S.; Kim, J. Carbonic Anhydrase for CO2 Capture, Conversion and Utilization. *Current Opinion in Biotechnology* **2022**, *74*, 230–240. https://doi.org/10.1016/j.copbio.2021.12.003.

(12)Liang, S.; Wu, X.-L.; Zong, M.-H.; Lou, W.-Y. Zn-Triazole Coordination Polymers: Bioinspired Carbonic Anhydrase Mimics for Hydration and Sequestration of CO2. *Chemical Engineering Journal* **2020**, *398*, 125530. https://doi.org/10.1016/j.cej.2020.125530.

(13)Verma, M.; Bhaduri, G. A.; Phani Kumar, V. S.; Deshpande, P. A. Biomimetic Catalysis of CO_2 Hydration: A Materials Perspective. *Industrial & Engineering Chemistry Research* **2021**, *60* (13), 4777–4793. https://doi.org/10.1021/acs.iecr.0c06203.

(14)Floyd, W. C.; Baker, S. E.; Valdez, C. A.; Stolaroff, J. K.; Bearinger, J. P.; Satcher, J. H.; Aines, R. D. Evaluation of a Carbonic Anhydrase Mimic for Industrial Carbon Capture. *Environmental Science & Technology* **2013**, *47* (17), 10049–10055. https://doi.org/10.1021/es401336f.

(15)Saeed, M.; Deng, L. CO2 Facilitated Transport Membrane Promoted by Mimic Enzyme. *Journal of Membrane Science* **2015**, *494*, 196–204. https://doi.org/10.1016/j.memsci.2015.07.028.

(16)Zhu, Y.; Li, W.; Sun, G.; Tang, Q.; Bian, H. Enzymatic Properties of Immobilized Carbonic Anhydrase and the Biocatalyst for Promoting CO 2 Capture in Vertical Reactor. *International journal of greenhouse gas control* **2016**, *49*, 290–296. https://doi.org/10.1016/j.ijggc.2016.03.016.

(17)Zhang, Y.; Zhu, J.; Hou, J.; Yi, S.; Van, B.; Zhang, Y. Carbonic Anhydrase Membranes for Carbon Capture and Storage. *Journal of Membrane Science Letters* **2022**, *2* (2), 100031–100031. https://doi.org/10.1016/j.memlet.2022.100031.

(18)Oleksii Zozulia; Dolan, M. A.; Korendovych, I. V. Catalytic Peptide Assemblies. *Chemical Society Reviews* **2018**, *47* (10), 3621–3639. https://doi.org/10.1039/c8cs00080h.

(19)Jin, H.; Jiao, F.; Daily, M. D.; Chen, Y.; Yan, F.; Ding, Y.-H.; Zhang, X.; Robertson, E. J.; Baer, M. D.; Chen, C.-L. Highly Stable and Self-Repairing Membrane-Mimetic 2D Nanomaterials Assembled from Lipid-like Peptoids. *Nature Communications* **2016**, *7* (1). https://doi.org/10.1038/ncomms12252.

(20)Jin, H.; Ding, Y.; Wang, M.; Song, Y.; Liao, Z.; Newcomb, C. J.; Wu, X.; Tang, X.-Q.; Li, Z.; Lin, Y.; Yan, F.; Jian, T.; Mu, P.; Chen, C.-L. Designable and Dynamic Single-Walled Stiff Nanotubes Assembled from Sequence-Defined Peptoids. *Nature Communications* **2018**, *9* (1).

https://doi.org/10.1038/s41467-017-02059-1.

(21) Zheng, R. *et al.* Assembly of short amphiphilic peptoids into nanohelices with controllable supramolecular chirality. *Nat. Commun.* **15**, 3264 (2024). https://doi.org:10.1038/s41467-024-46839-y

(22) Shao, L. *et al.* Hierarchical Self-Assembly of Multidimensional Functional Materials from Sequence-Defined Peptoids. *Angew. Chem., Int. Ed.* **63**, e202403263 (2024). https://doi.org:https://doi.org/10.1002/anie.202403263

(23) Trinh, T. K. H. *et al.* Designed Metal-Containing Peptoid Membranes as Enzyme Mimetics for Catalytic Organophosphate Degradation. *ACS Appl. Mater. Interfaces* **15**, 51191-51203 (2023). https://doi.org:10.1021/acsami.3c11816

(24) Shao, L. *et al.* Hierarchical Materials from High Information Content Macromolecular Building Blocks: Construction, Dynamic Interventions, and Prediction. *Chem. Rev.* **122**, 17397-17478 (2022). https://doi.org:10.1021/acs.chemrev.2c00220

(25) Jian, T. *et al.* Highly stable and tunable peptoid/hemin enzymatic mimetics with natural peroxidase-like activities. *Nat. Commun.* **13**, 3025 (2022). https://doi.org:10.1038/s41467-022-30285-9

26) Li, Z., Cai, B., Yang, W. & Chen, C.-L. Hierarchical Nanomaterials Assembled from Peptoids and Other Sequence-Defined Synthetic

Polymers. *Chem. Rev.* **121**, 14031-14087 (2021). https://doi.org:10.1021/acs.chemrev.1c00024

(27) Cai, B., Li, Z. & Chen, C.-L. Programming Amphiphilic Peptoid Oligomers for Hierarchical Assembly and Inorganic Crystallization. *Acc. Chem. Res.* **54**, 81-91 (2021). https://doi.org:10.1021/acs.accounts.0c00533

(28)Kim, T.; Jian, T.; Jin, B.; Nguyen, D.-T.; Zuckermann, R. N.; Chen, C.-L. Designed Metal-Containing Peptoid Membranes as Enzyme Mimetics for Catalytic Organophosphate Degradation. *ACS Applied Materials & Interfaces* **2023**, *15* (44), 51191–51203. https://doi.org/10.1021/acsami.3c11816.

(29)Pierre, A. C. Enzymatic Carbon Dioxide Capture. *ISRN Chemical Engineering* **2012**, *2012*, 1–22. https://doi.org/10.5402/2012/753687.

(30)Shao, L.; Hu, D.; Zheng, S.; Trinh, T. K. H.; Zhou, W.; Wang, H.; Zong, Y.; Li, C.; Chen, C. Hierarchical Self-Assembly of Multidimensional Functional Materials from Sequence-Defined Peptoids. *Angewandte Chemie International Edition* **2024**, *63* (24). https://doi.org/10.1002/anie.202403263.

(31)Zhang, C.; Shafi, R.; Lampel, A.; MacPherson, D.; Pappas, C. G.; Narang, V.; Wang, T.; Maldarelli, C.; Ulijn, R. V. Switchable Hydrolase

Based on Reversible Formation of Supramolecular Catalytic Site Using a Self-Assembling Peptide. *Angewandte Chemie International Edition* **2017**, *56* (46), 14511–14515. https://doi.org/10.1002/anie.201708036.

(32)Liao, Y.; Sheridan, T. R.; Liu, J.; Lu, Z.; Ma, K.; Yang, H.; Farha, O. K.; Hupp, J. T. Probing the Mechanism of Hydrolytic Degradation of Nerve Agent Simulant with Zirconium-Based Metal–Organic Frameworks. *ACS Catalysis* **2023**, *14* (1), 437–448. https://doi.org/10.1021/acscatal.3c04469.

(33)Song, Y. *et al.* Highly Bright and Photostable Two-Dimensional Nanomaterials Assembled from Sequence-Defined Peptoids. *ACS Mater. Lett.* **3**, 420-427 (2021). https://doi.org:10.1021/acsmaterialslett.1c00110.

(34)Luo, Y. *et al.* Bioinspired Peptoid Nanotubes for Targeted Tumor Cell Imaging and Chemo-Photodynamic Therapy. *Small* **15**, 1902485 (2019). https://doi.org:10.1002/smll.201902485.